AN AUTOMATED PROCEDURE FOR MATERIAL PARAMETER EVALUATION FOR VISCOPLASTIC CONSTITUTIVE MODELS

P.K. Imbrie, G.H. James, P.S. Hill,
D.H. Allen, and W.E. Haisler
Texas A&M University
College Station, Texas 77843

An automated procedure is presented for evaluating the material parameters in Walker's exponential viscoplastic constitutive model for metals at elevated temperature. Both physical and numerical approximations are utilized to compute the constants for Inconel 718 at 1100°F. When intermediate results are carefully scrutinized and engineering judgement applied, parameters may be computed which yield stress output histories that are in agreement with experimental results. A qualitative assessment of the θ-plot method for predicting the limiting value of stress is also presented. The procedure may also be used as a basis to develop evaluation schemes for other viscoplastic constitutive theories of this type.

INTRODUCTION

A large number of unified viscoplastic theories are currently being developed for metals[1]. These models generally require the evaluation of numerous material parameters before they can be utilized. These constants are highly coupled to one another, and, due to the nonlinearity and stiffness of the governing equations, they are difficult to evaluate. The evaluation of these parameters is normally accomplished in a heuristic way due to the complexity of the models, so that the values of the constants are dependent on the person evaluating them. The purpose of this research was to develop an automated procedure for the evaluation of material parameters utilized in Walker's exponential viscoplastic constitutive model for metals at elevated temperature[2,3]. The procedure developed herein entails a synthesis of physical and numerical approximations which use various combinations of experimental data, as well as engineering intuition to determine the constants. The impetus for this work was two-fold. First, automated procedures for determining the material parameters are needed if standardized material parameters are ever to be realized. Second, in order to improve the present theories, a thorough understanding of the approximations and/or assumptions made during their development and subsequent usage is required.

While the model developed by Walker is only one of many currently being used, similarities are notable in a number of other theories such as those proposed by Krieg, Swearengen, and Rhode[4], Bodner[3], and Schmidt and Miller[5]. Therefore, it is believed by these authors that the general procedure presented herein may be applied to other models such as those mentioned above.

THE MODEL

The model proposed by Walker is a viscoplastic theory which uses a flow law for the inelastic strain rate, which is an exponential in stress. The growth law modeling back stress is of the hardening/recovery form and accounts for both dynamic and static thermal recovery. The drag stress term models isotropic hardening, thus accounting for the cyclic hardening or softening characteristics of metals. The uniaxial differential form of Walker's exponential model may be written as:

$$\dot{\varepsilon}^I = \frac{\exp(\frac{\sigma - B}{D}) - 1}{\beta} \operatorname{sgn}(\sigma - B) \quad , \tag{1}$$

$$\dot{B} = n_2 \dot{\varepsilon}^I - B\{|n_3 + n_4 \exp(-n_5 |\log(\frac{\dot{R}}{\dot{R}_0})|| \dot{R} + n_6\}, \tag{2}$$

$$D = D_1 - D_2 \exp(-n_7 R) \quad , \tag{3}$$

$$\dot{R} = |\dot{\varepsilon}^I| \quad , \tag{4}$$

where σ is the applied stress, ε^I is the inelastic strain, B is the back stress, and D is the drag stress. A superposed dot above the variables denotes differentiation with respect to time. The material parameters for this model are β, n_2, n_3, n_4, n_5, n_6, n_7, D_1, and D_2 . Therefore, nine constants need to be evaluated, in addition to Young's Modulus E and the strain aging parameter R_0 . These same constants are required for the multiaxial formulation, in addition to Poisson's ratio.

The experiments required to determine the constants for Walker's model using the procedure developed herein include: 1) A series of constant strain rate steady state hysteresis loops under fully reversed strain controlled conditions (Fig. 1); 2) cyclic hold tests performed on the unloading branch of the cyclic tests (Fig.2); and 3) long term monotonic tension tests (Fig. 3).

The cyclic hold tests are used to measure the back stress and are performed by cycling a material until saturated conditions are reached. Hold times are then inserted at various points in the unloading region as shown in Fig. 2. If the test frame is in load control, then the back stress is equal to the applied stress when no creep is observed for a given hold time.

The monotonic tension and cyclic hold tests are used to evaluate the material parameters found in the inelastic strain rate equation and the back stress growth law, whereas the cyclic hysteresis tests are used primarily to obtain constants for the isotropic hardening variable. The monotonic tests may not be necessary if acceptable values of the limiting stress (σ_{lim}) can be obtained from the first half cycle of the cyclic tests. The aforementioned experiments were performed on Inconel 718 at 1100° F. A complete description of the test procedures and results may be found in reference [6].

DETERMINATION OF THE CONSTANTS

The procedure for determining the material parameters in Walker's theory is described in the ensuing paragraphs. The equations, which are a result of both physical and numerical approximations, can be coalesced into a single interactive computer code. Since approximations are made, from time to time the user may have to judiciously select some constants in order to complete the constant calculation process. The reason for this can be an insufficient data base, poor experimental results, or a material response that the model cannot handle.

Evaluation of the material parameters begins by plotting σ_{lim} versus $\ln(\dot{\varepsilon}^I)$. A nonlinear representation signifies that strain aging and/or thermal recovery effects are present and thus need to be modeled. If σ_{lim} is not obtained experimentally, it can be estimated in a manner similar to that

proposed by Lindholm, et al.[2].

If σ_{lim} is to be estimated, then under conditions of uniaxial tension loading, when $\dot{\varepsilon}^I$ is assumed to be a constant and equal to the applied strain rate and $\exp(\frac{\sigma-B}{D}) >> 1$,eq. (1) may be written as:

$$\sigma = D \ln (\beta\dot{\varepsilon}^I) + B \quad . \tag{5}$$

Using the evolution equation defining the back stress (eq. (2)) and the assumption that D remains constant during monotonic loading, then $d\sigma/d\varepsilon^I$ (or θ) may be written as:

$$\theta = n_2 - \beta[n_3 + n_4\exp(-n_5|\log(\frac{\dot{R}}{\dot{R}_0})|) + n_6/\dot{\varepsilon}^I] \quad . \tag{6}$$

Thus, equations (5) and (6) can be combined, yielding

$$\theta = -N\sigma + [n_2 + ND\ln(\beta\dot{\varepsilon}^I)] \quad , \tag{7}$$

where

$$N = n_3 + n_4 \exp(-n_5|\log(\frac{\dot{R}}{\dot{R}_0})|) + n_6/\dot{\varepsilon}^I \quad . \tag{8}$$

Therefore, equation (7) indicates that a plot of θ versus σ should be linear at low inelastic strains, having a slope of N and an x-intercept of σ_{lim} . The θ- plot is obtained by plotting stress versus inelastic strain (as shown in Fig. 4(a)) to find $\sigma(\varepsilon^I)$, which in general is a n^{th} order polynomial. This function is then numerically differentiated and plotted versus stress to produce the θ- plot (see Fig. 4(b)). Hence, values of N and σ_{lim} can be

obtained for each monotonic tension test using a linear regression scheme. If acceptable values of σ_{1im} are obtained experimentally, the θ- plot may still be used to determine N. In this situation, the linear fit results in a slope which is forced to pass through σ_{1im} .

The constant n_5 is computed by determining where the effect of strain aging is considered negligible and may be written as:

$$n_5 = -[\ln(\tau)/|\log(\frac{\dot{R}_1}{\dot{R}_0})|] \quad . \tag{9}$$

The constants $\dot{R}_0$ and $\dot{R}_1$ represent the strain rate at which the strain aging correction is a maximum and minimum, respectively, and τ denotes the residual correction at rate $\dot{R}_1$. It should be noted that τ also affects the rate of decay of the strain aging correction and selection of too small a value will result in a very localized correction.

The next step in this procedure is to compute the dynamic and static thermal recovery constants n_3, n_4, and n_6 using equation (8). Assuming that a limiting value of stress has been obtained, then $\dot{\varepsilon}=\dot{\varepsilon}^I$ and eq. (8) can be written a number of times, corresponding to the different monotonic tests (denoted by the subscript i) as:

$$N_i = n_3 + n_4 f_i + n_6/\dot{\varepsilon}_i^I \quad , \tag{10}$$

where

$$f_i = \exp(-n_5|\log(\frac{\dot{R}_i}{\dot{R}_0})|) \quad . \tag{11}$$

Thus, the three parameters n_3, n_4, and n_6 may be obtained simultaneously

using a multiple linear regression scheme. A plot of this curve fit will indicate if acceptable values of the dynamic and thermal recovery parameters have been found. In the event that poor results are obtained (as shown in Fig.5) , one of the following actions can be taken: 1) The data base can be scrutinized more carefully, using additional tests to capture the desired effect or deleting tests that do not appear consistent; 2) values of n_3, n_4, and n_6 can be assigned using engineering intuition; or 3) an uncoupled method (to be discussed below) for evaluating the constants can be used.

The uncoupled formulation assumes that thermal recovery effects can be neglected for high strain rate tests. Thus, eq. (10) may be written as:

$$N_i = n_3 + n_4 f_i \quad . \tag{12}$$

Therefore, n_3 and n_4 can be computed by a linear least squares algorithm where n_3 is the intercept and n_4 is the slope (see Fig. 5). If this method is used, the constant n_6 should be initially set to zero and determined later in the procedure.

The hardening coefficient n_2 is computed on the basis that B saturates to B_{lim} at large inelastic strains. Hence, $\dot{B}=0$ and equation (2) reduces to

$$B_{lim} = \frac{n_2}{n_3 + n_4 f + n_6/\dot{\varepsilon}^I} \quad . \tag{13}$$

If it is assumed that the ratio σ_{exp}/B_{exp} will remain constant for the limiting condition at sufficiently large inelastic strains, then

$$\frac{\sigma_{exp}}{B_{exp}} = \frac{\sigma_{lim}}{B_{lim}} \quad . \tag{14}$$

Substituting eq. (13) into (14) and solving for n_2 results in

$$n_2 = \frac{[n_3 + n_4 f + n_6/\dot{\varepsilon}^I]\sigma_{lim}}{\sigma_{exp}} \cdot \frac{B_{exp}}{\sigma_{exp}} \quad , \tag{15}$$

where σ_{lim} values are obtained from long term monotonic tension tests or θ-plots and B_{exp}/σ_{exp} values come from cyclic hold tests. The final value of the hardening coefficient is then computed as the arithmetic mean of the number of experiments. If an acceptable value of n_2 is not obtained, it can be specified, noting that this parameter effects the rate of hardening.

The initial value of drag stress D_0 and the inelastic strain rate scalar β are determined by rewriting equation (15) using the limiting values of σ and B as:

$$\sigma_{lim} - B_{lim} = D_0 \ln(\dot{\varepsilon}^I) + D_0 \ln(\beta) \ . \tag{16}$$

Since B_{lim} is given by equation (13), it can be substituted into equation (16), resulting in

$$\delta_{\sigma B} \equiv \sigma_{lim} - \frac{n_2}{n_3 + n_4 f + n_6/\dot{\varepsilon}^I} = D_0 \ln(\dot{\varepsilon}^I) + D_0 \ln(\beta) \quad . \tag{17}$$

Equation (17) indicates that a plot of $\delta_{\sigma B}$ versus $\ln(\dot{\varepsilon}^I)$ should be linear (the piecewise curve shown in Fig. 6 is an artifact of the strain aging correction in the dynamic recovery term of the back stress evolution equation), having a slope of D_0 and an intercept of D $\ln(\beta)$ which are obtained from a linear regression analysis. Hence, β can be computed directly once the

value of the intercept is known.

If thermal recovery effects were previously neglected, the constant n_6 can now be evaluated. Since β and D_0, n_2, n_3, and n_4 are known, eq. (13) can be substituted into eq. (16) yielding an expression for n_6 :

$$n_6 = \dot{\varepsilon}^I \{n_2 [\sigma_{lim} - D_0 \ln(\beta\dot{\varepsilon}^I)]^{-1} - n_3 - n_4 f\} \quad . \tag{18}$$

The thermal recovery parameter is then computed for a number of low strain rate monotonic tension tests and averaged.

Up to this point, the only tests that are needed in order to compute the material parameters are monotonic tension and cyclic hold tests. To obtain the isotropic hardening and recovery constants D_1, D_2, and n_7, saturated cyclic hysteresis data are required. By estimating the cumulative inelastic strain from applied stress, strain amplitude, and E, in addition to assuming that D saturates to D_1 , then n_7 can be approximated by:

$$n_7 = -\ln(\tau)/R_{avg} \quad , \tag{19}$$

where R_{avg} is the average of R for a number of tests and τ is a number approaching zero.

On the physical basis that B saturates much more rapidly than D, equation (5) can be written as:

$$D_{lim} = D_1 = \frac{\sigma_{lim} - B_{lim}}{\ln(\beta\dot{\varepsilon}^I)} \quad , \tag{20}$$

where

$$B_{lim} = n_2/N \quad . \tag{21}$$

The values of σ_{lim} and N in equations (20) and (21) are estimated from the θ-plot using data from the tension half-cycle after cyclic saturation has occurred. If several tests are used, D_1 is computed as the arithmetic mean.

The final parameter to be determined is D_2 . When R=0 equation (3) reduces to

$$D_0 = D_1 - D_2 \ , \tag{22}$$

from which D_2 may be computed directly, completing the constant calculation procedure.

The primary equations used in the procedure described above are summerized below and a flow chart of the associated computer code is shown in Fig. 7. The program is written to compute the constants in a totally automated fashion or, alternately, the parameters can be modified and/or recomputed through user intervention. While the flow chart depicts the procedure as a sequential series of evaluations, the user may alter the program flow to iterate on a specific constant or series of constants.

1) Values of σ_{lim} and N from monotonic tension tests are computed using equation (7) and a least squares procedure.
2) After selecting $\dot{R}_0$, $\dot{R}_1$, and τ, n_5 is evaluated using equation (9).
3) The parameters n_3, n_4, and n_6 are determined, in a coupled formulation, by equations (10) and (11) using a multiple linear regression scheme, or

alternately, using an uncoupled formulation by equations (12) and (18).

4) The back stress hardening coefficient n_2 is computed directly from equation (15).

5) The constants D_0 and β are evaluated using equation (17) via a least squares procedure.

6) After computing the cumulative inelastic strain from the experimental data, n_7 is evaluated directly from equation (19).

7) D_1 and D_2 are computed using equation (20) and (22).

DISCUSSION OF THE PROCEDURE AND RESULTS

The parameter evaluation program, described in the previous section, does not require an entire experimental data base. Instead, summary information which is composed of both measured quantities and pre-processed values is all that is necessary. Data tabulated from fully reversed cyclic tests, cyclic hold tests and long term monotonic tension tests on Inconel 718 at 1100° F may be found in Table 1. These data were used to compute an initial set of constants (see Table 2) in a totally automated fashion. Comparisons between Walker's exponential model and several tension experiments may be seen in Fig.'s 8-10. It is apparent that the initial set of parameters did not enable the model to capture the true response of the material. Therefore, a critical review of both the procedure and experimental data was necessary.

For the purpose of this discussion, it was assumed that the data base accurately represented the material behavior. Therefore, steps in the

procedure which require user interpretation were examined first and the following observations were made.

When constructing the θ-plot, there are several points to consider. First, proper evaluation of σ_{lim} and N require that ϵ^I be computed after $\dot{\epsilon}^I$ becomes constant. This is generally assumed to occur at the 0.2% offset yield stress. However, if this is not true, the computed value of N will be too large, which in turn will yield a value of σ_{lim} that is too low. A second area of interest is in the differentiation of the σ versus ϵ^I curve. Usually the stress is expressed as an nth order polynomial function of the inelastic strain. However, depending upon the viscoplastic model and material system, a logarithmic, power law or exponential curve fit may be more suitable. In addition, a finite difference approximation can be used, thus eliminating the curve fitting requirement altogether. Since a poor curve fit will yield a θ-plot that is difficult to interpret, care should be taken in selecting the proper form of the equation. Lastly, one needs to consider the strain amplitude necessary to obtain an accurate prediction of σ_{lim}.

The θ-plots for the material system considered herein were constructed using a combination of third and fourth order polynominal curve fits (see Fig. 4). Figure 11 shows that the values of N are scattered and have no specific trends when they are plotted against $\ln(\dot{\epsilon})$. In a similar fashion, Fig. 12 shows anomalies in the prediction of σ_{lim}. While the sigmoidal shape of the curve was expected, the large discrepancies make interpretation difficult.

To illustrate how scatter such as that depicted in Fig.'s 11 and 12 can occur, consider the following points. First, Fig. 13 shows a θ-plot constructed using a fourth order polynomial curve fit, evaluating $\sigma(\epsilon^I)$ over various strain amplitudes. While there is only a 6% change in

predicted σ_{lim}, there is over a 50% change in N. Some of the discrepancy can be attributed to the fact that $\dot{\varepsilon}^I$ was not constant. In addition, the order of the curve fit drastically changed the shape of the θ-plot making interpretation difficult . Second, Fig. 14 shows a θ-plot generated from a logarithmic curve fit. While not shown, evaluation of σ_{lim} and N over different strain amplitudes did not adversely affect their values. Finally, Fig. 15 depicts a θ-plot constructed using finite differences. It is apparent that numerical differentiation by this method yields unacceptable results. In summary, one must carefully consider both the constitutive model and material system before selecting the type of curve fit that will be used in the construction of the θ-plot.

It was also determined that the multiple linear regression scheme used to compute dynamic and static thermal recovery constants in a coupled fashion did not work well when the material exhibited substantial strain aging. Therefore, by neglecting thermal recovery, n_3 and n_4 were computed using an uncoupled procedure. Figures 8 through 10 show that Walker's model, using the final parameters (see Table 2), was able to reproduce the input data fairly well except in the initial yield region. Test 80 showed the largest deviation between actual and predicted stress, underestimating it by 6% at a strain amplitude of 0.8%.

Figures 16 through 18 show the model behavior for the last cycle of several cyclic hysteresis tests. Figures 17 and 18 indicate that the computed value of D_1 was too large, which resulted in an excess of material softening under cyclic loading. However, the opposite trend can be seen in Fig. 16 (test 86 was the fastest cyclic test run), wherein the peak stress amplitude was overpredicted. A review of the monotonic tension data reveals the same tendency. This would lead to the conclusion that the full effect of the

strain aging correction was not captured.

A complex history test (one which was not used to evaluate the constants) was used to show the predictive capabilities of Walker's model using the final set of parameters. In general, Fig. 19 indicates the numerical simulation matches the test fairly well. The only major problem encountered was a 7.5% overprediction in stress at large strain amplitudes.

CONCLUSIONS

A method for obtaining the material parameters for Walker's model has been developed which is a synthesis of both physical and numerical approximations. The associated computer algorithm allows the user to specify either a totally automated procedure or engineering intuition at selected points when computing constants. In addition, qualitative assessments were made regarding the use of the θ-plot in determining σ_{lim} and N. It was noted that the method of differentiating the σ versus ε^I curve depends on both the constitutive model being used and the material system.

Walker's viscoplastic constitutive model for metals at elevated temperature was compared to experiment results for Inconel 718 at 1100°F. This material system responds with apparent strain aging, undergoes cyclic work softening, and is susceptible to low cycle fatigue. It was shown that Walker's model was able to capture the response of the material. It has also been shown that the use of the linearized equations can lead to unacceptable simulations if care is not used to interpret the results. The procedure yields initial values for the constants which may then be used in an iterative scheme to arrive at the final parameters.

REFERENCES

1. D.H. Allen, and J.M. Beek, "On the Use of Internal State Variables in Thermoviscoplastic Constitutive Equations," Nonlinear Constitutive Relations for High Temperature Application - 1984, NASA CP 2369, pp. 83-102, 1984.

2. K.P. Walker and D.A. Wilson, "Creep Crack Growth Predictions in INCO 718 Using a Continuum Damage Model," 2nd Symposium on Nonlinear Constitutive Relations for High-Temperature Applications, Cleveland, OH, 1984.

3. U.S. Lindholm, K.S. Chan, S.R. Bodner, R.M., Weber, K.P. Walker, and B.N. Cassenti, "Constitutive Modeling for Isotropic Materials," CR-174980, NASA (Host), 1985.

4. R.D. Krieg, J.C. Swearengen, and R.W. Rhode, "A Physically-based Internal Variable Model for Rate Dependent Plasticity," Proc. ASME/CSSME PVP Conference, 1978.

5. C.G. Schmidt, A Unified Phenomenological Model for Solute Hardening, Strain Hardening, and Their Interactions in Type 316 Stainless Steel, Ph.D. Dissertation, Stanford University, Dept. of Materials Science and Engineering, 1979.

6. G.H. James III, "An Experimental Comparison of Current Viscoplastic Constitutive Models at Elevated Temperature, M.S. Thesis, Texas A&M University, 1986.

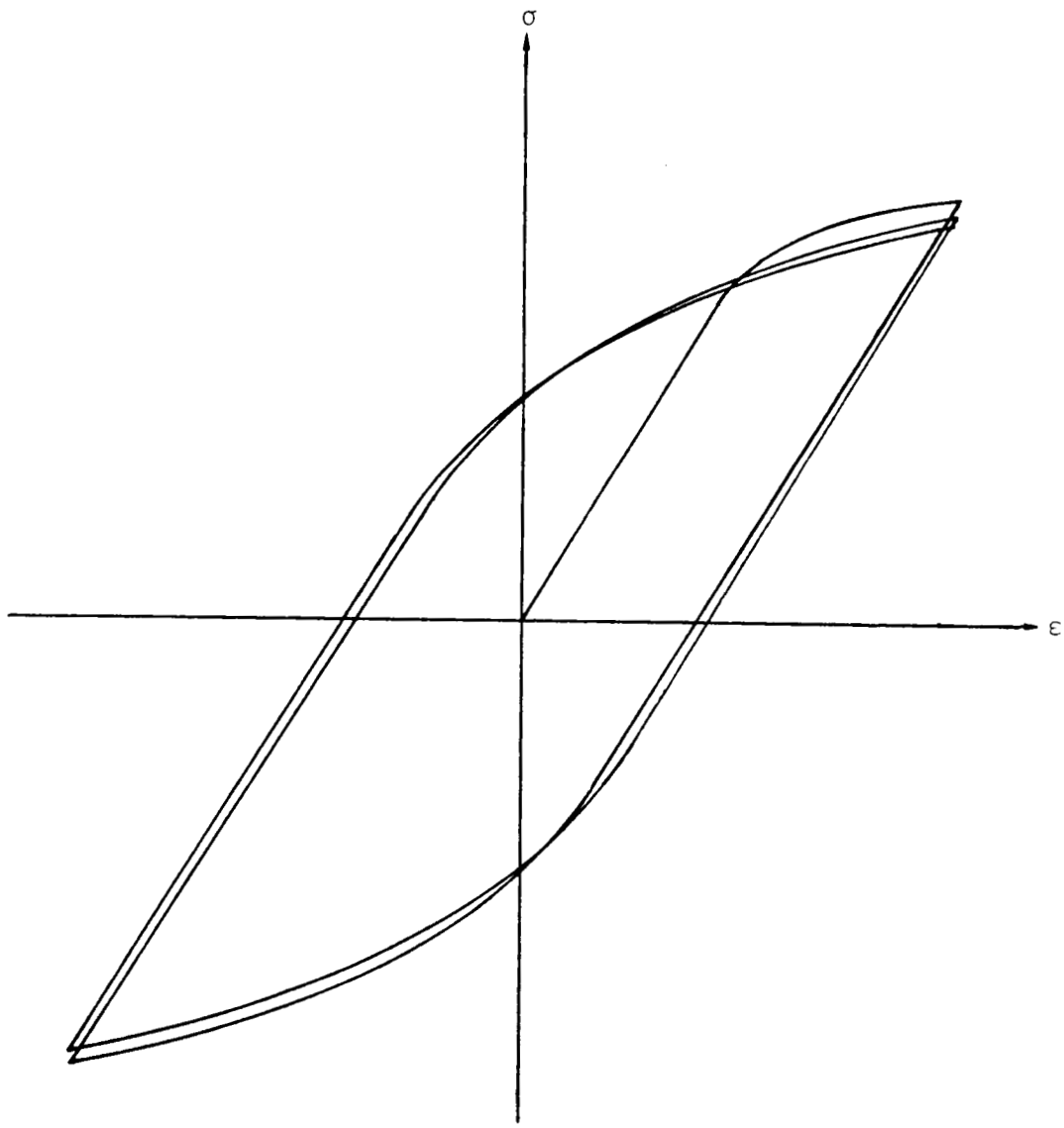

Figure 1. Cyclic Hysteresis Test

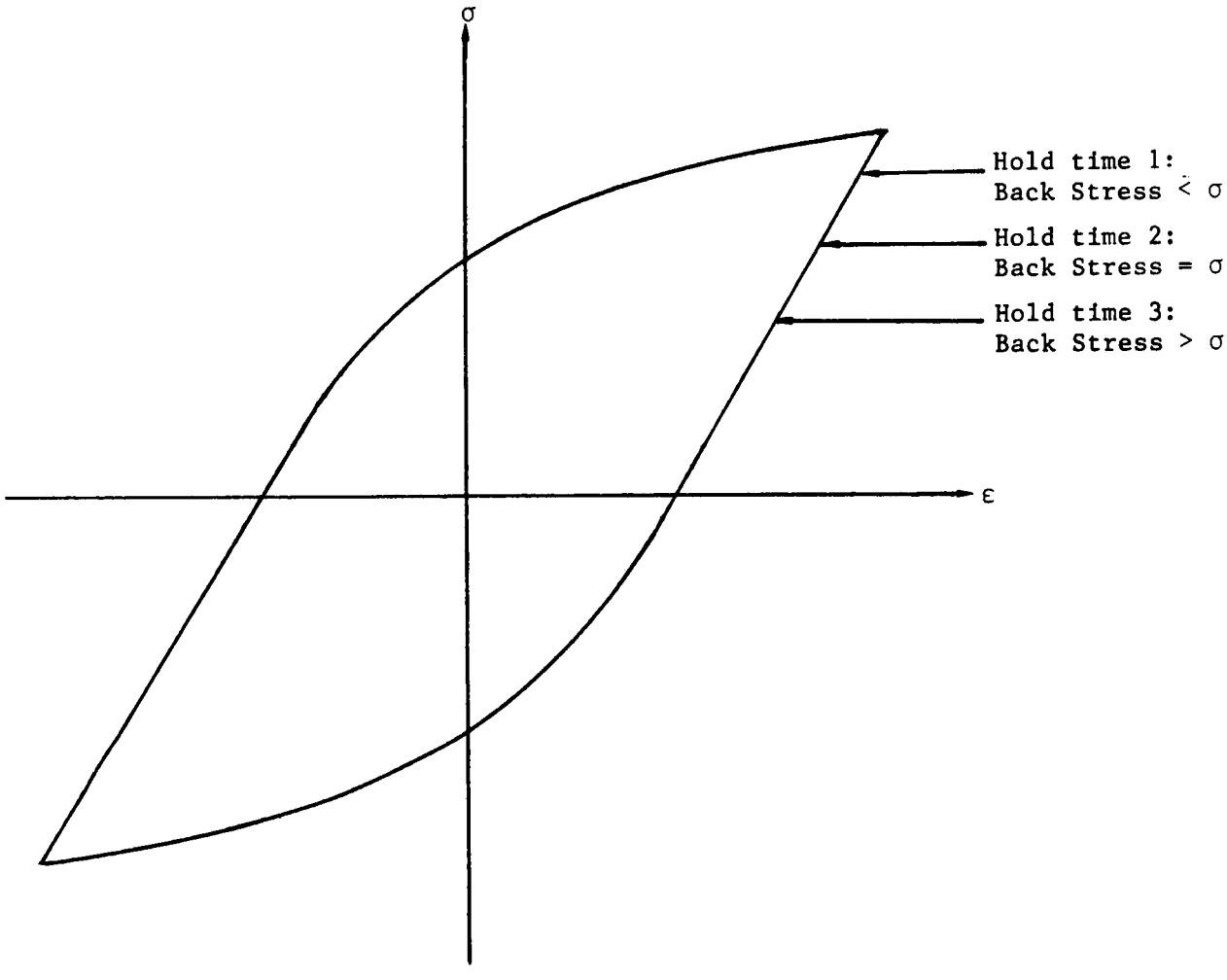

Figure 2. Cyclic Hysteresis Test with Hold Times

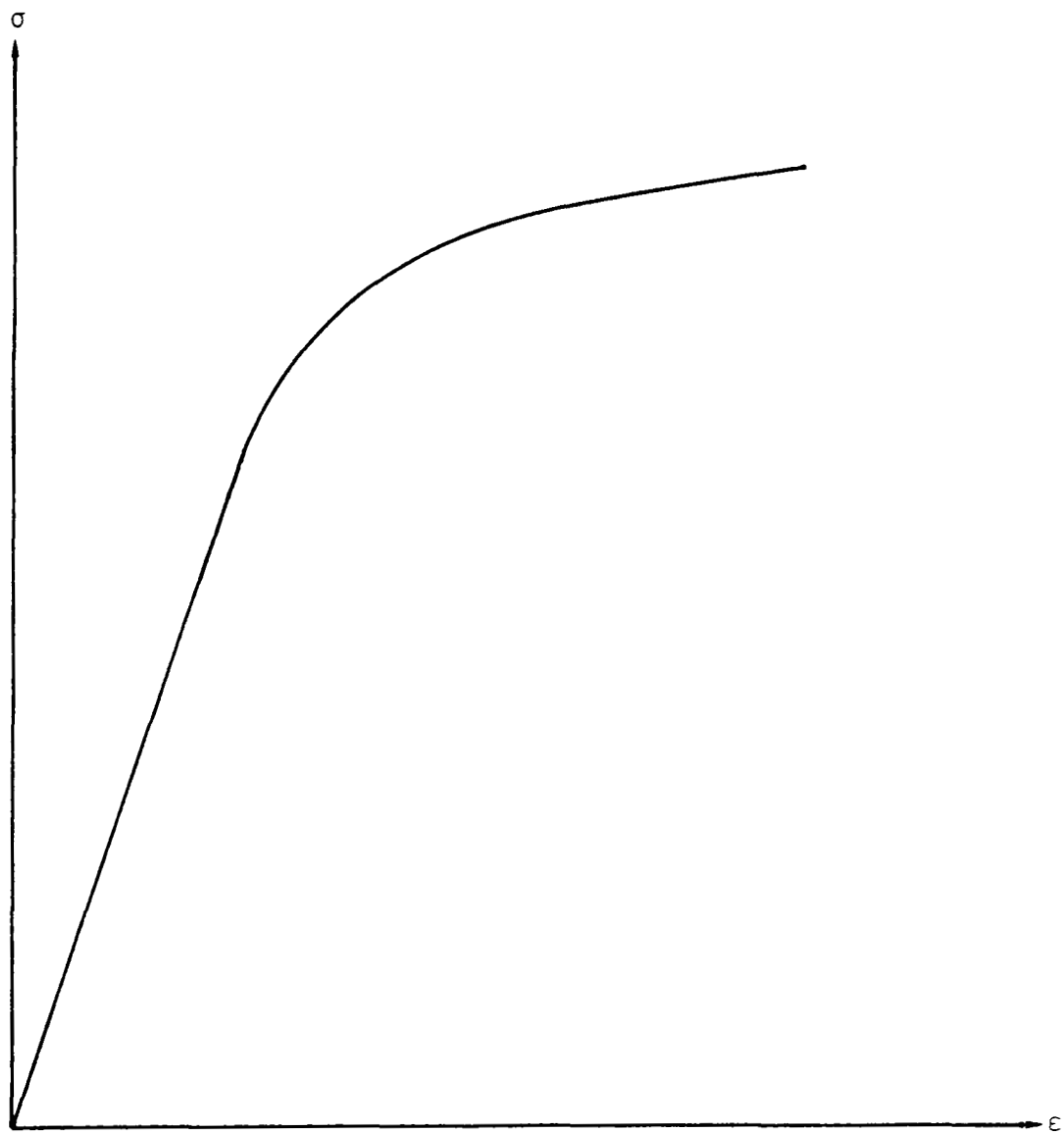

Figure 3. Long Term Monotonic Tension Test

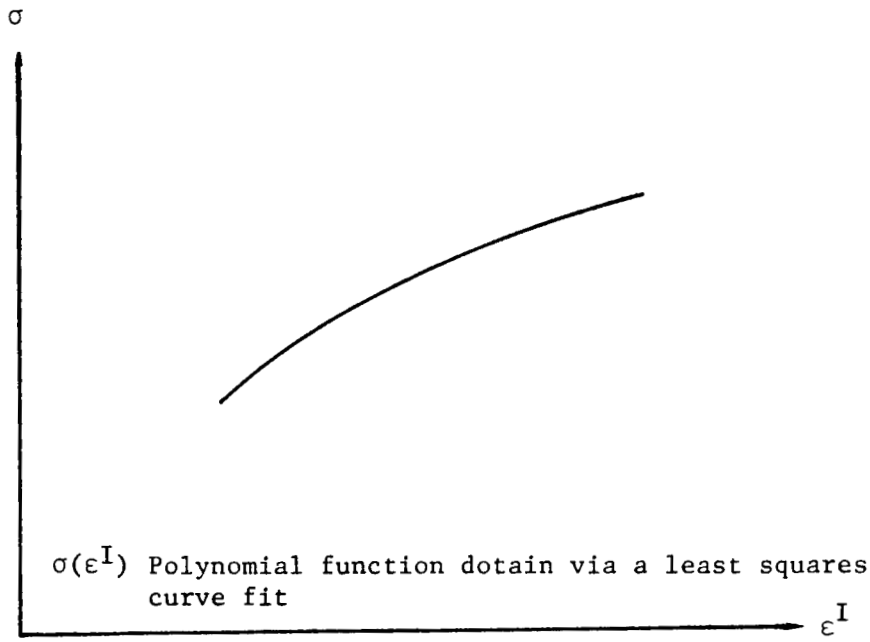

Figure 4(a). Stress versus inelastic strain

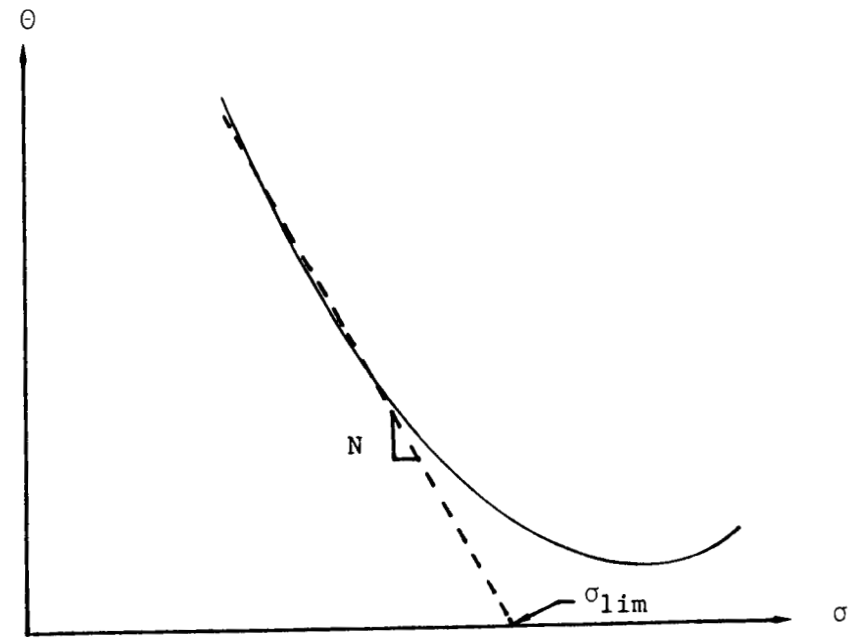

Figure 4(b). Typical Θ-plot

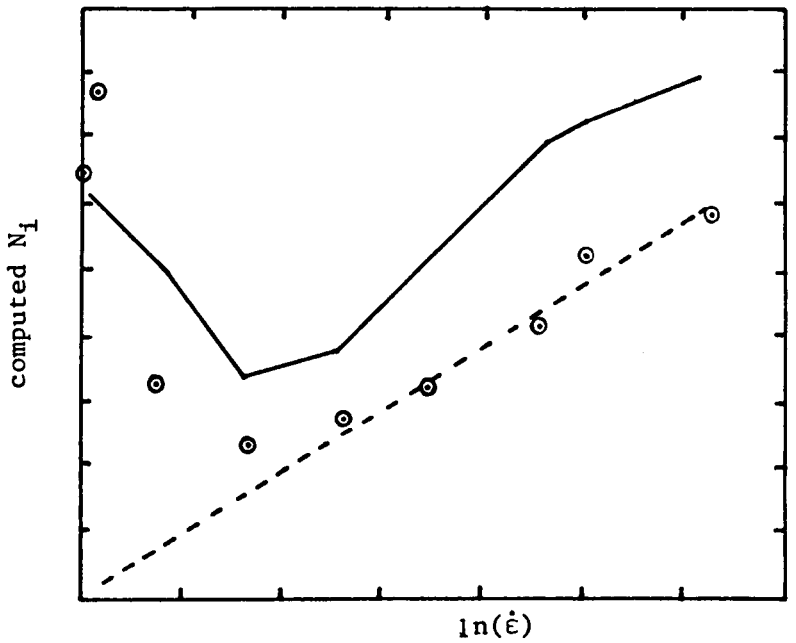

⊙ values of N obtained from the Θ-plots

—— n_3, n_4, and n_6 obtained simultaneously using a multiple linear regression scheme

- - - n_3 and n_4 computed using a linear regression scheme

Figure 5. Least squares fit of N as a function $\dot{\varepsilon}^I$ (note: the abscissa is shown as $\ln(\dot{\varepsilon})$ instead of $\dot{\varepsilon}$ for pictorial purposes only)

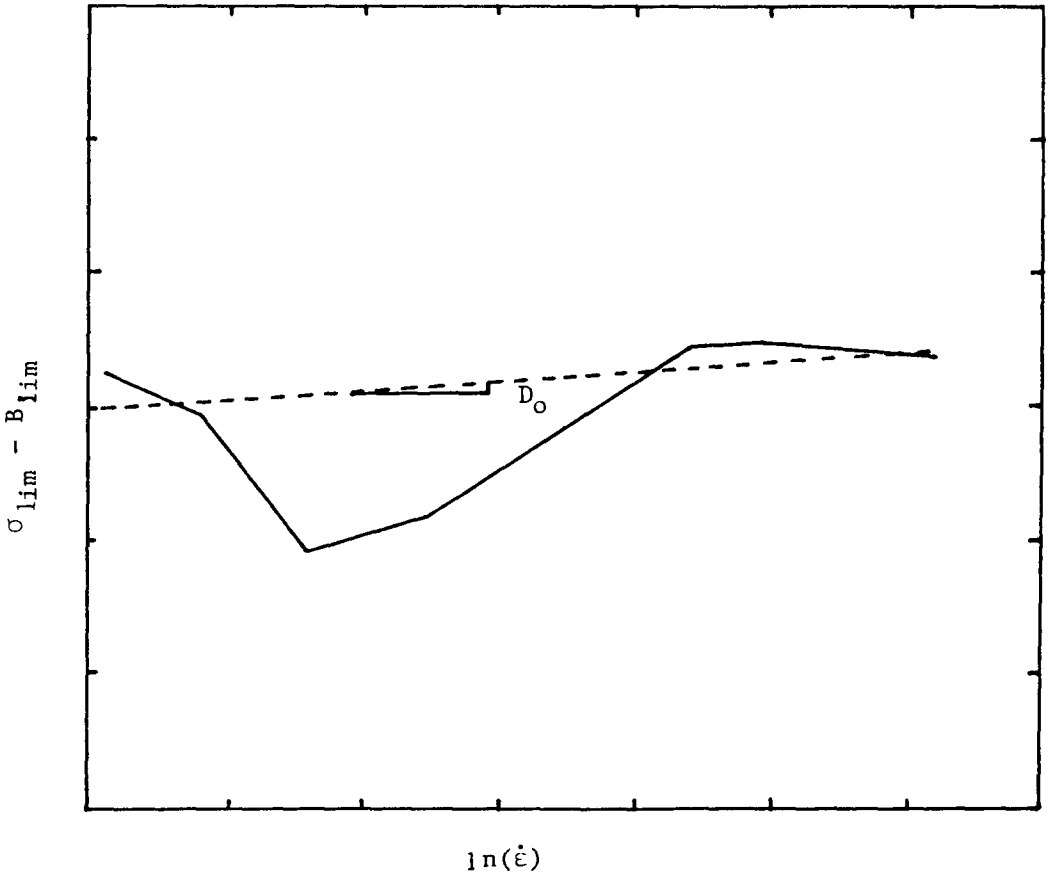

Data to be fit

Result of linear regression analysis

Figure 6. Least squares fit of $\delta_{\sigma B}$ as a function $\ln(\dot{\varepsilon}^I)$

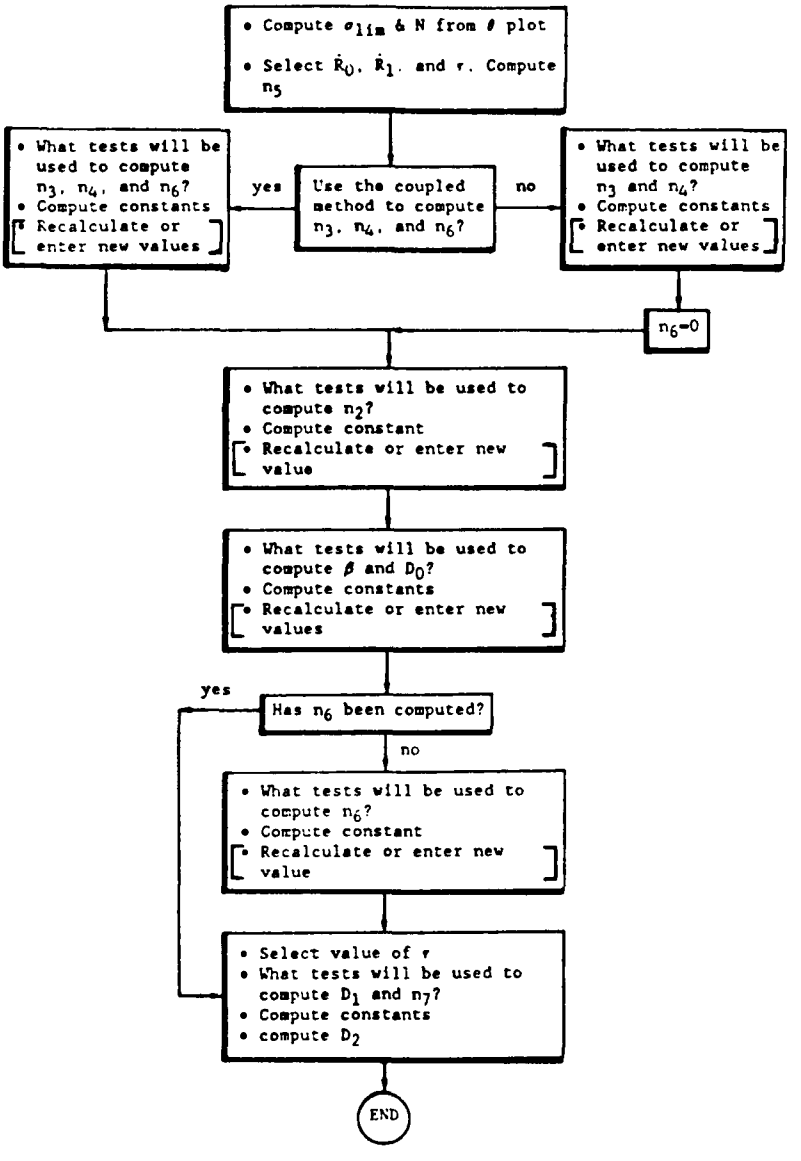

[ ] Modifications requiring user intervention

Figure 7. Flowchart of Walker's Procedure

Test No. P	E	$\dot{\varepsilon}$	σ_{exp}	σ_{lim}	σ_y	B_{exp}	N	R
1	70	3.151×10^{-3}		132.527	97.83		287.293	
2	86	1.002×10^{-4}		120.938	91.677		307.181	
3	56	9.966×10^{-4}		118.217	95.575		305.436	
* 4	35	9.235×10^{-4}		136.3			277.2	
* 5	37	6.948×10^{-4}		137.5			246.9	
6	65	3.127×10^{-4}		134.143	97.84		268.17	
* 7	39	$1.793\times10^{-}$		130.6			206.61	
8	83	9.926×10^{-5}		134.536	94.56		337.399	
* 9	34	7.637×10^{-5}		142.1			319.8	
* 10	36	5.703×10^{-5}		138.5			241.6	
11	80	3.054×10^{-5}		141.821	100.941		310.777	
* 12	42	1.914×10^{-5}		137.6			291.8	
* 13	38	1.410×10^{-5}		140.7			212.4	
14	72	7.626×10^{-6}		138.155	101.71		358.549	
15	71	7.253×10^{-6}		135.584	97.67		342.254	
* 16	40	7.029×10^{-6}		138.3			328.5	
17	84	2.812×10^{-3}	116.48	132.527		68.3		
18	88	9.272×10^{-4}	100.98	120.938		62.47		
19	88	9.272×10^{-4}	100.98	118.217		62.47		
20	81	8.635×10^{-4}	116.45	120.938		64.65		
21	81	8.635×10^{-4}	116.45	118.217		64.65		
22	65	2.751×10^{-4}	107.84	134.143		80.00		
23	86	1.002×10^{-3}		108.326			288.42	0.0773
24	56	9.966×10^{-4}		105.897			294.58	0.0799
25	65	3.127×10^{-4}		121.427			248.02	0.0707
26	83	9.926×10^{-5}		136.699			267.179	0.0293
27	80	3.054×10^{-5}		135.899			255.534	0.0578
28	72	7.262×10^{-6}		139.38			375.035	0.0205

* Different Material System

Table 1. Input Data for Parameter Evaluation

Parameters	Initial Values	Final Values
β (sec)	0.288E34	0.280E70
D_1 (ksi)	0.580E00	0.520E00
D_2 (ksi)	-0.000E00	-0.120E00
$\dot{\epsilon}_o^I$ in/in/sec	0.454E-4	0.454E-4
E (ksi)	0.247E05	0.247E05
n_2 (ksi)	0.264E05	0.140E05
n_3	0.370E03	0.390E03
n_4	-0.200E03	-0.200E03
n_5	0.530E00	0.103E01
n_6 (/sec)	0.400E-4	0.400D-4
n_7 (/sec)	0.179E02	0.179E02

Table 2. Parameters for Walker's model

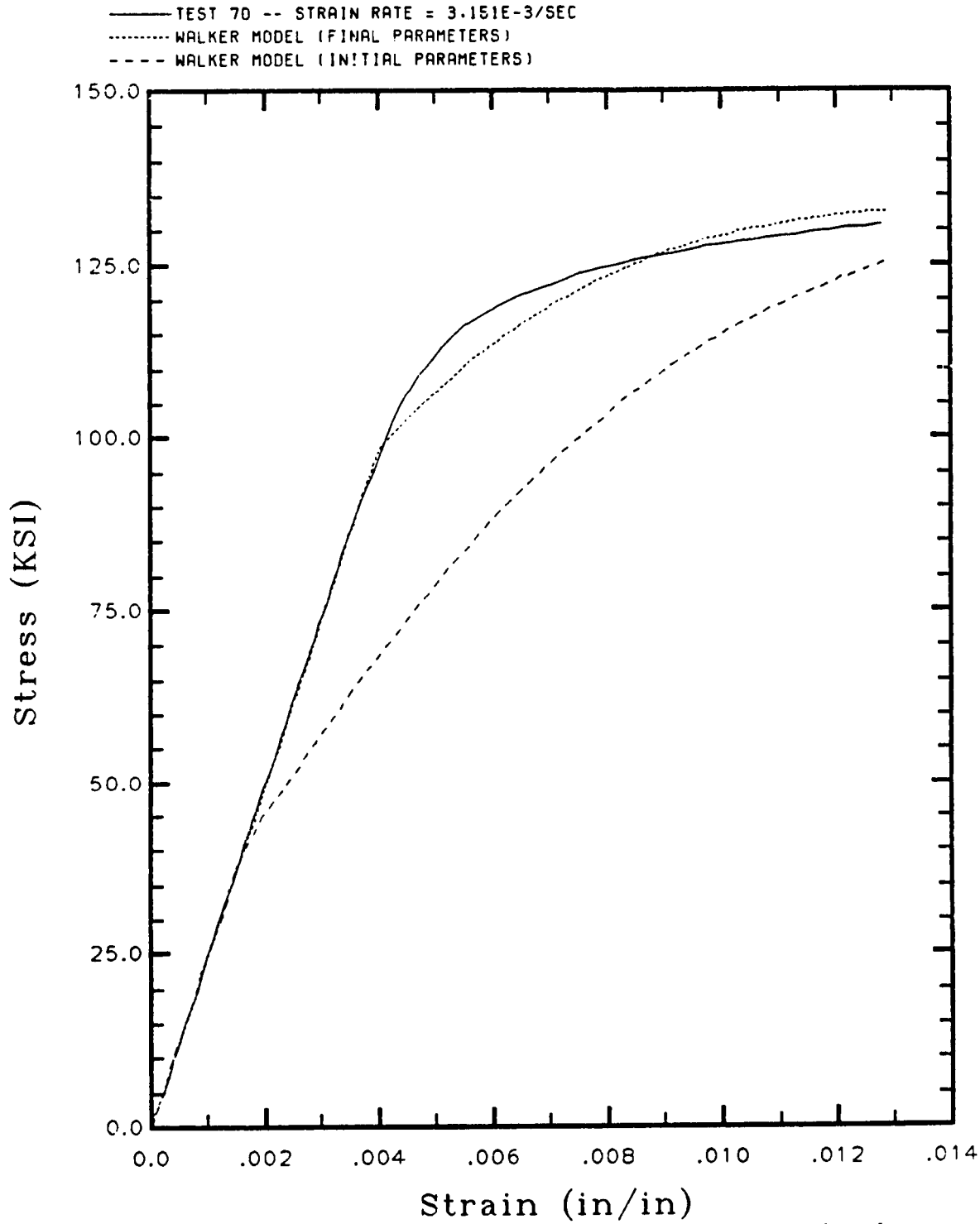

Figure 8. Comparison of Walker's model with initial and final parameters to Test 70-a long term monotonic tension test.

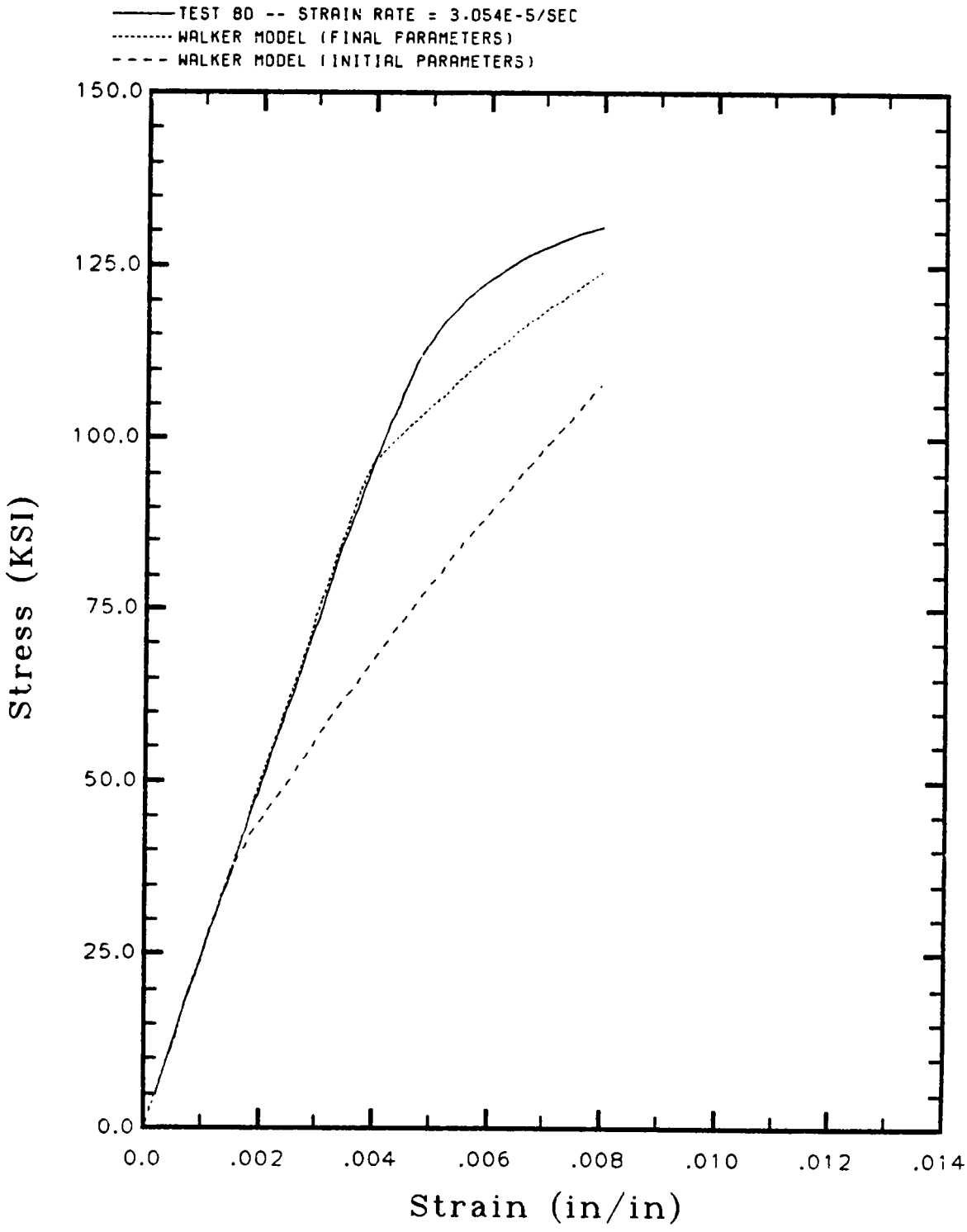

Figure 9. Comparison of Walker's model with initial and final parameters to Test 80-a short term monotonic tension test.

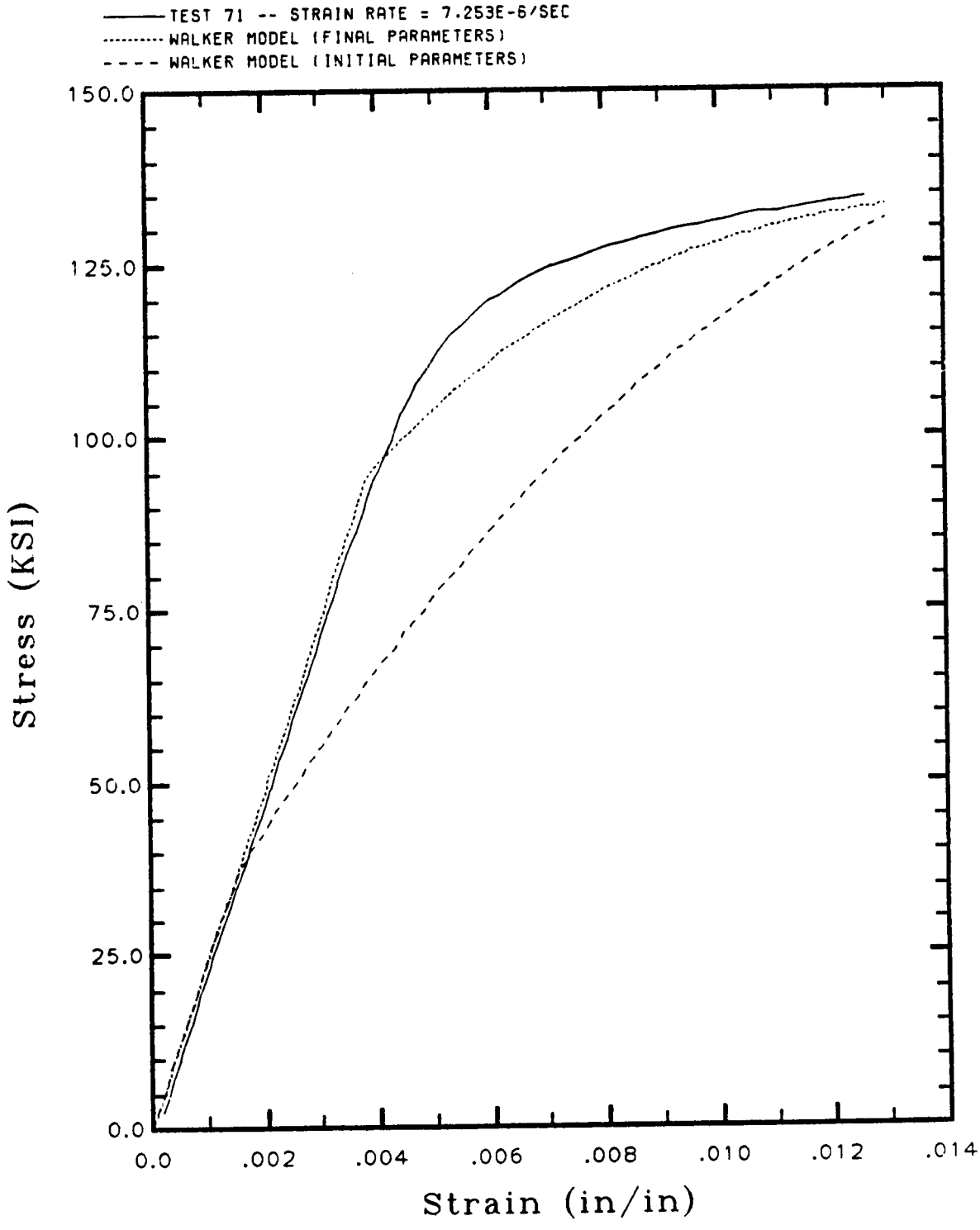

Figure 10. Comparison of Walker's model with initial and final parameters to Test 71-a long term monotonic tension test.

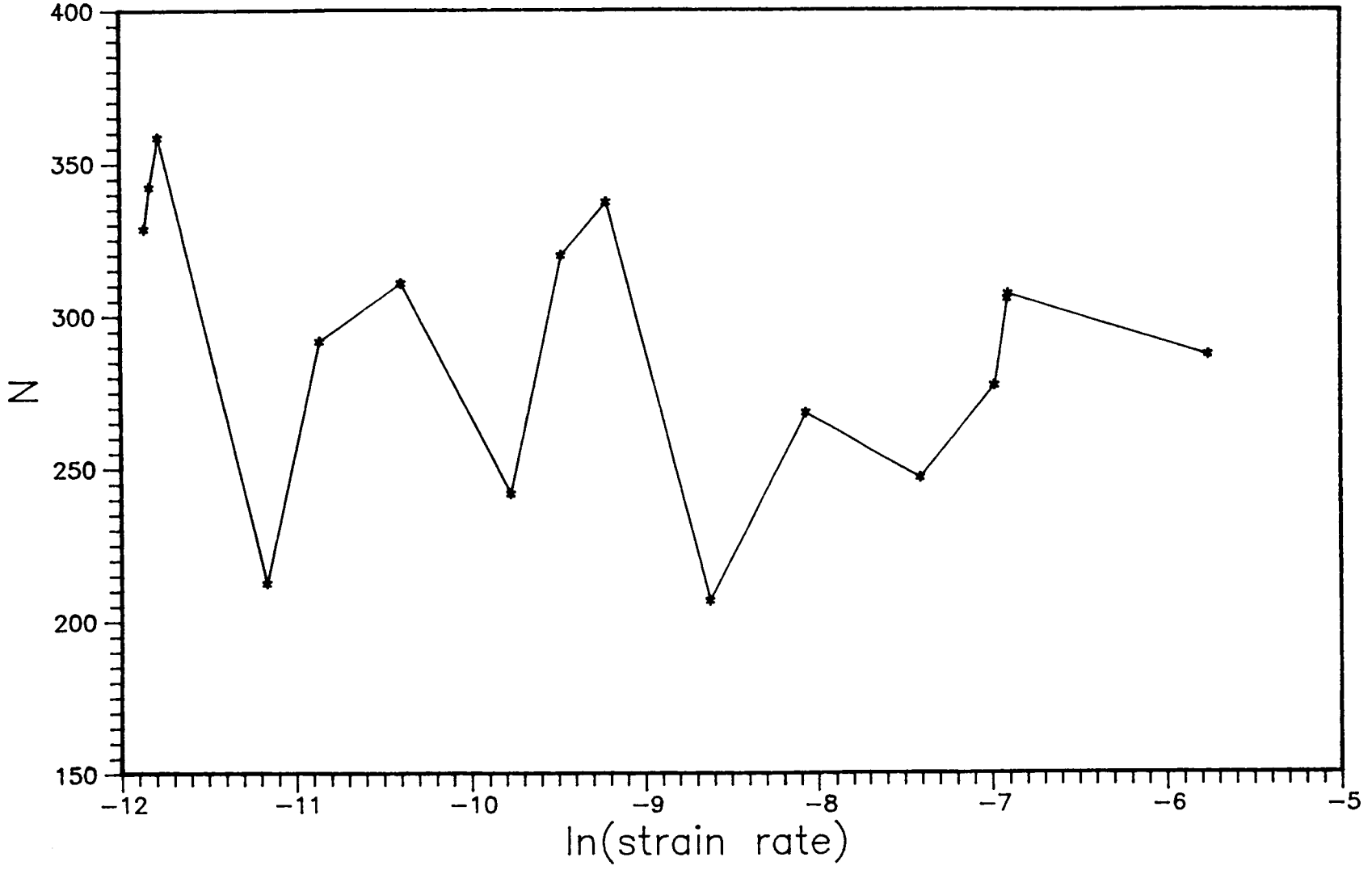

Figure 11. Computed values of N from the Θ-plot

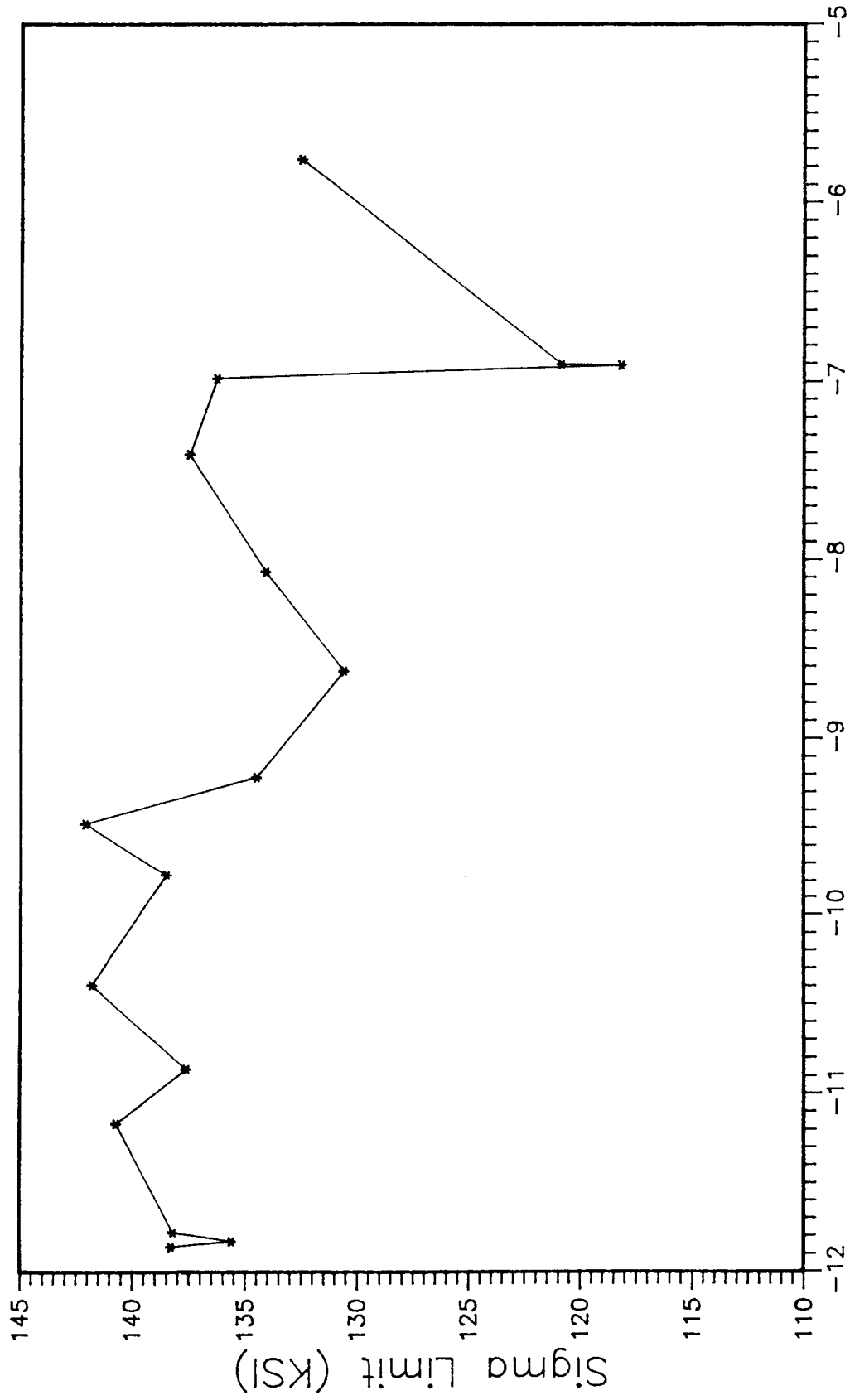

Figure 12. Predicted σ_{lim} from the Θ-plot

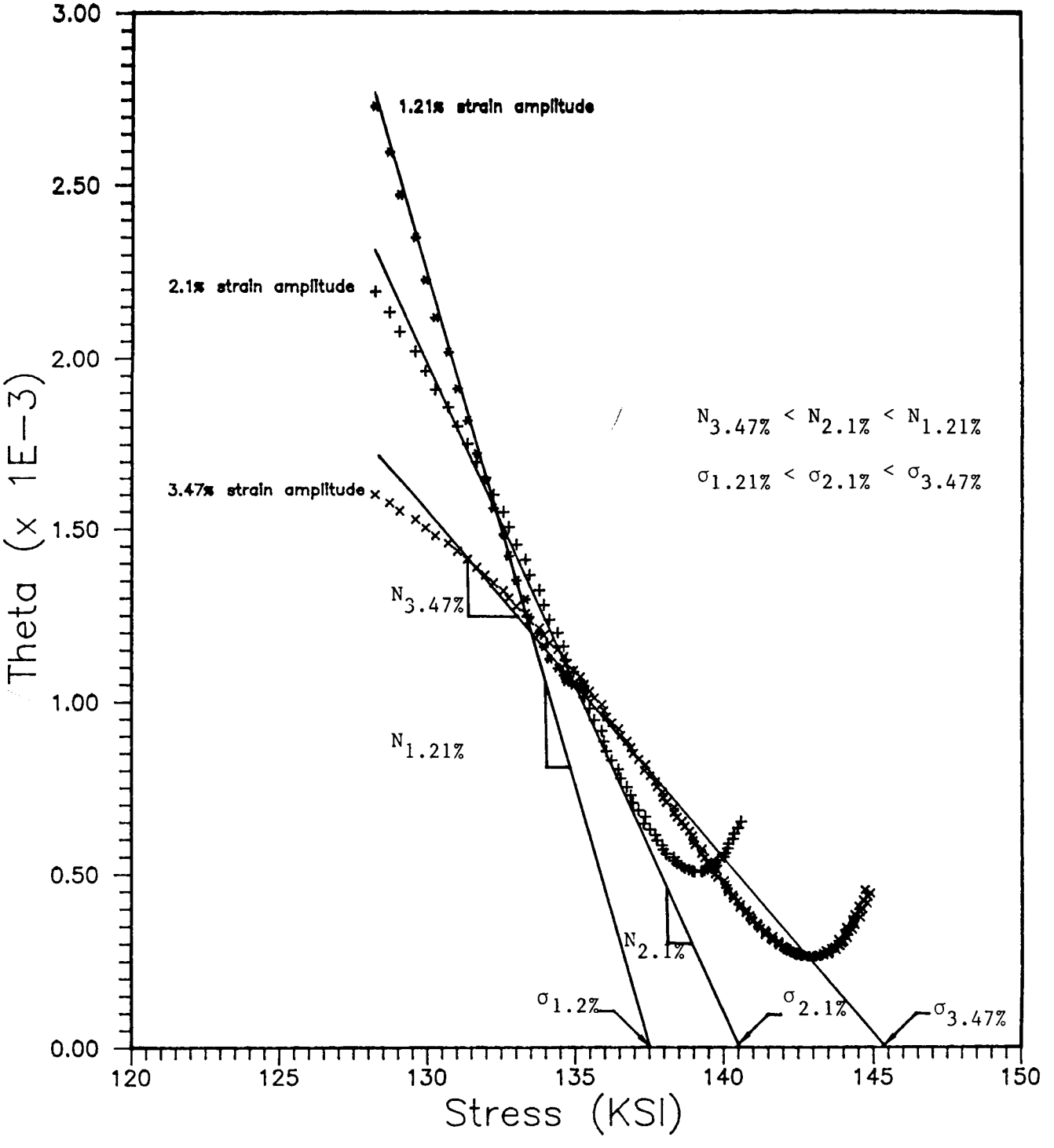

Figure 13. Θ-plot using a 4th order polynomial fit, evaluating $\sigma(\varepsilon^I)$ over different strain amplitudes

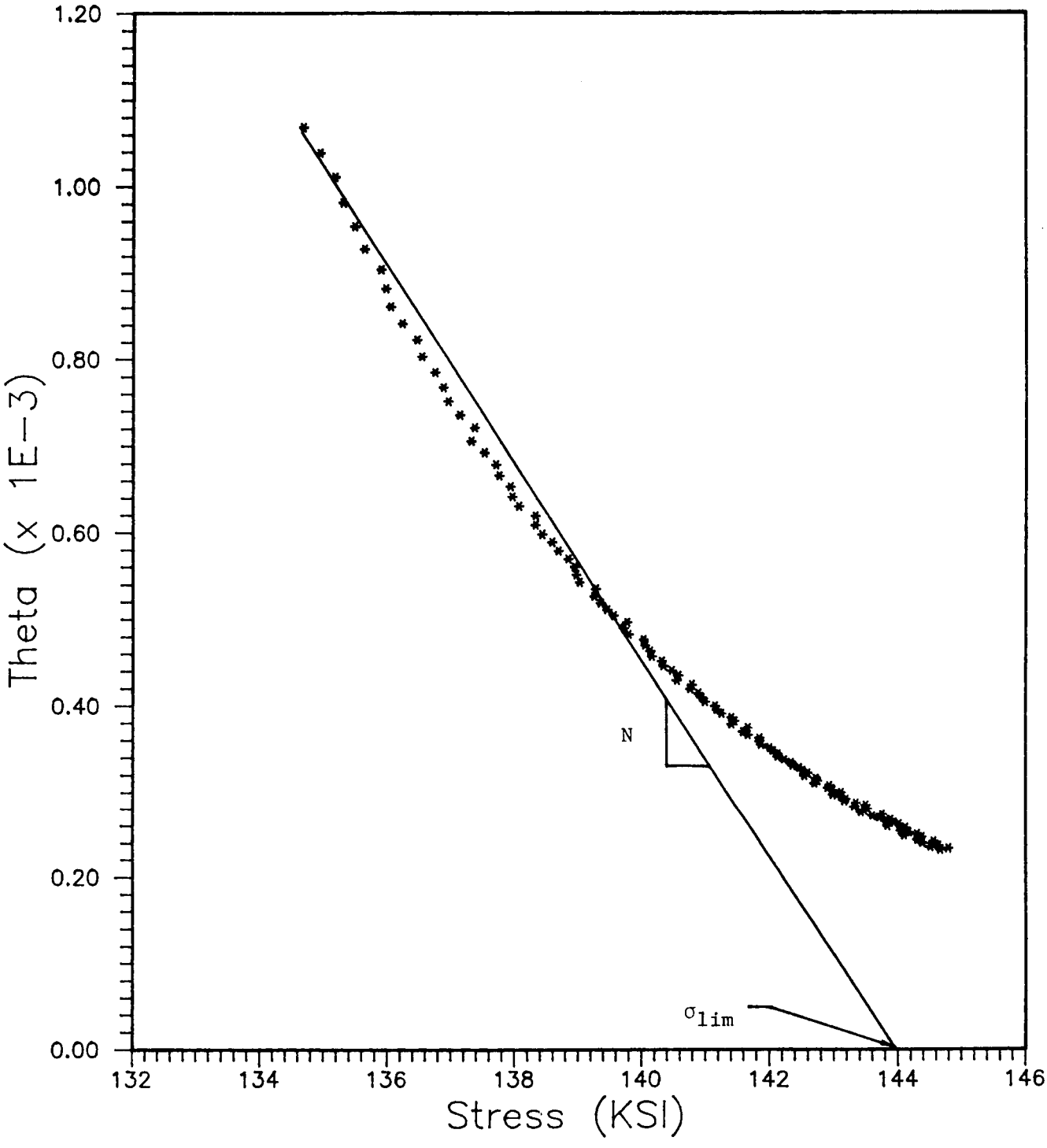

Figure 14. Θ-plot using a logarithmic curve fit of σ vs ε^I

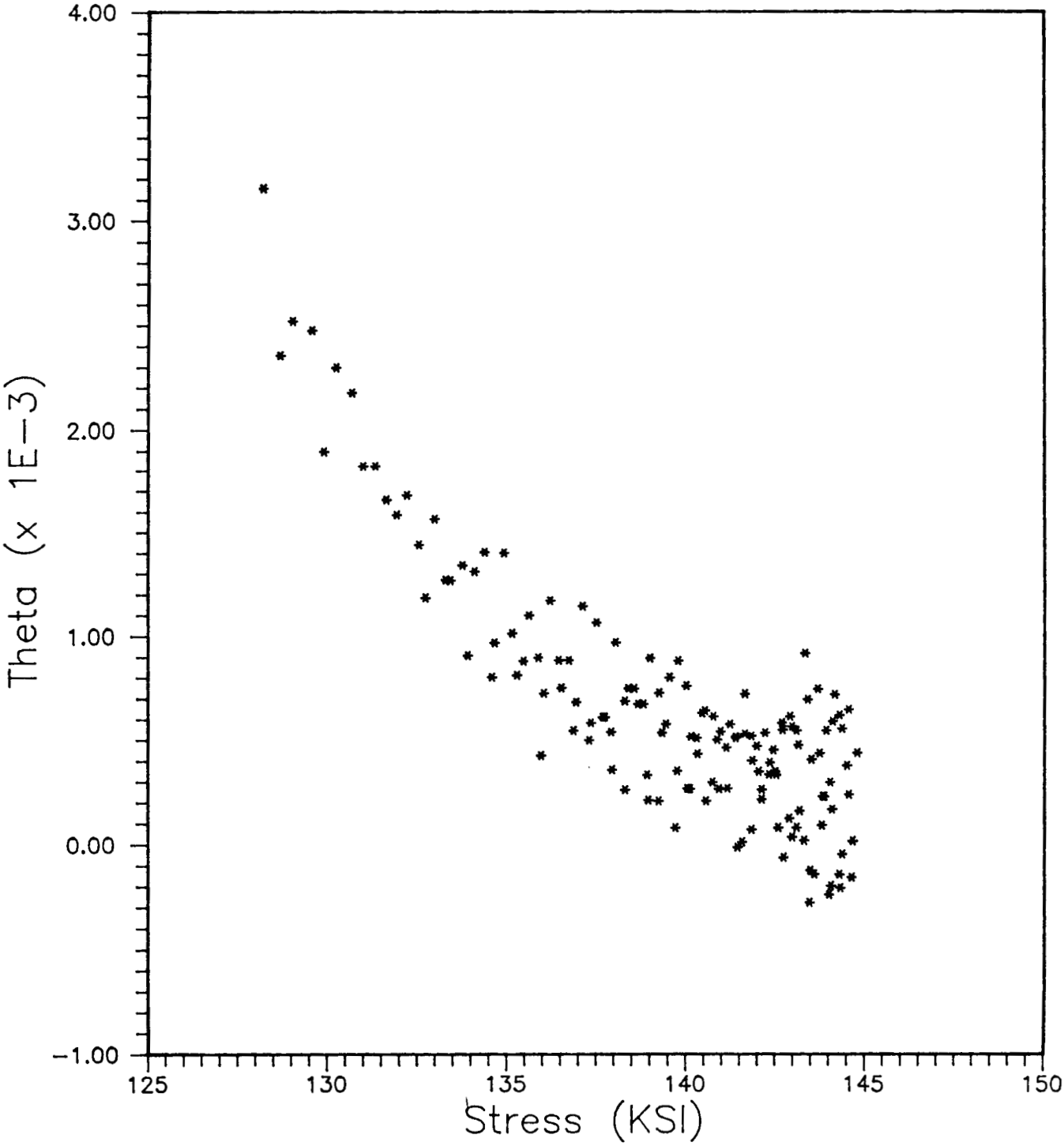

Figure 15. Θ-plot constructed by finite difference

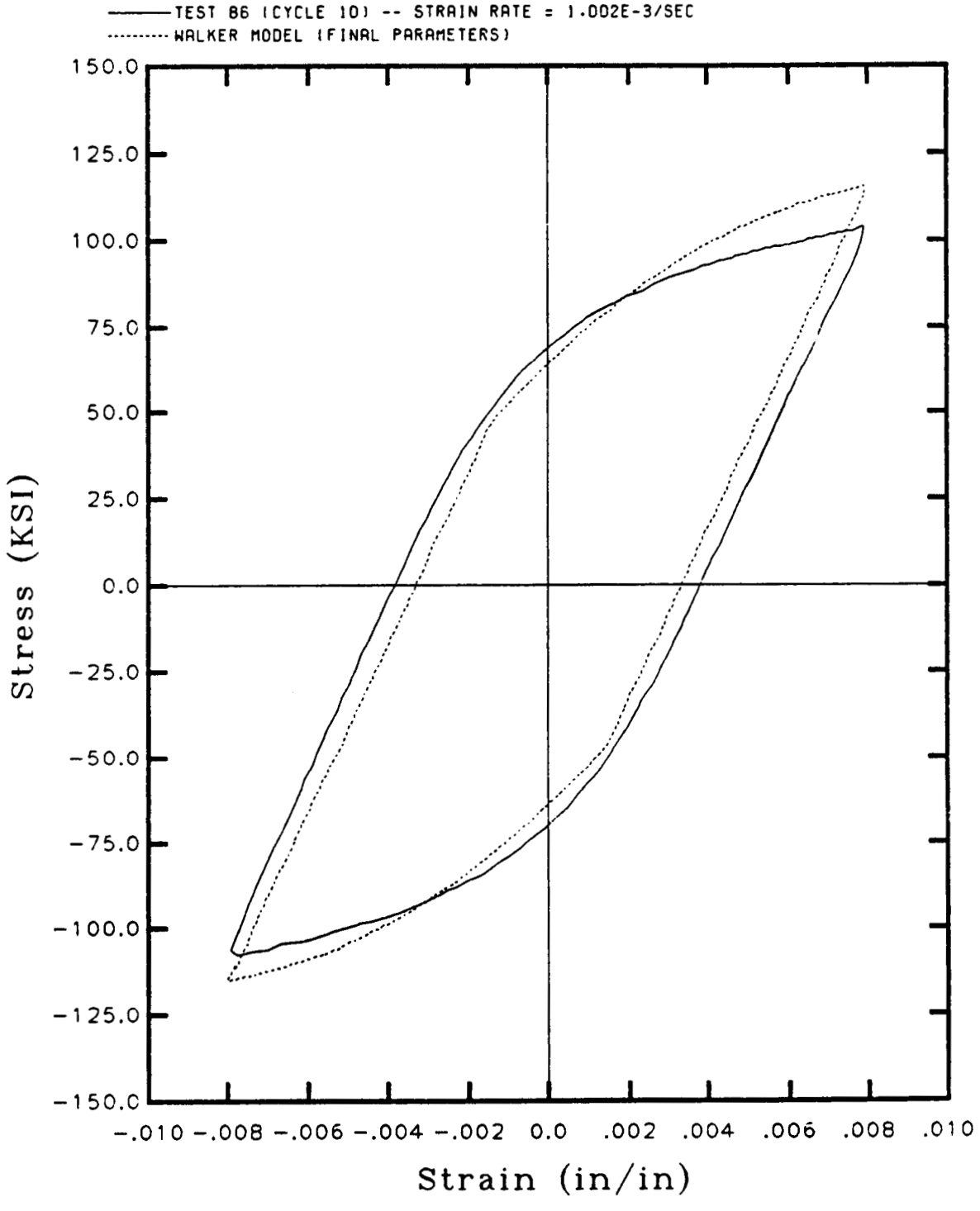

Figure 16. Comparison of Walker's model to the last cycle of Test 86.

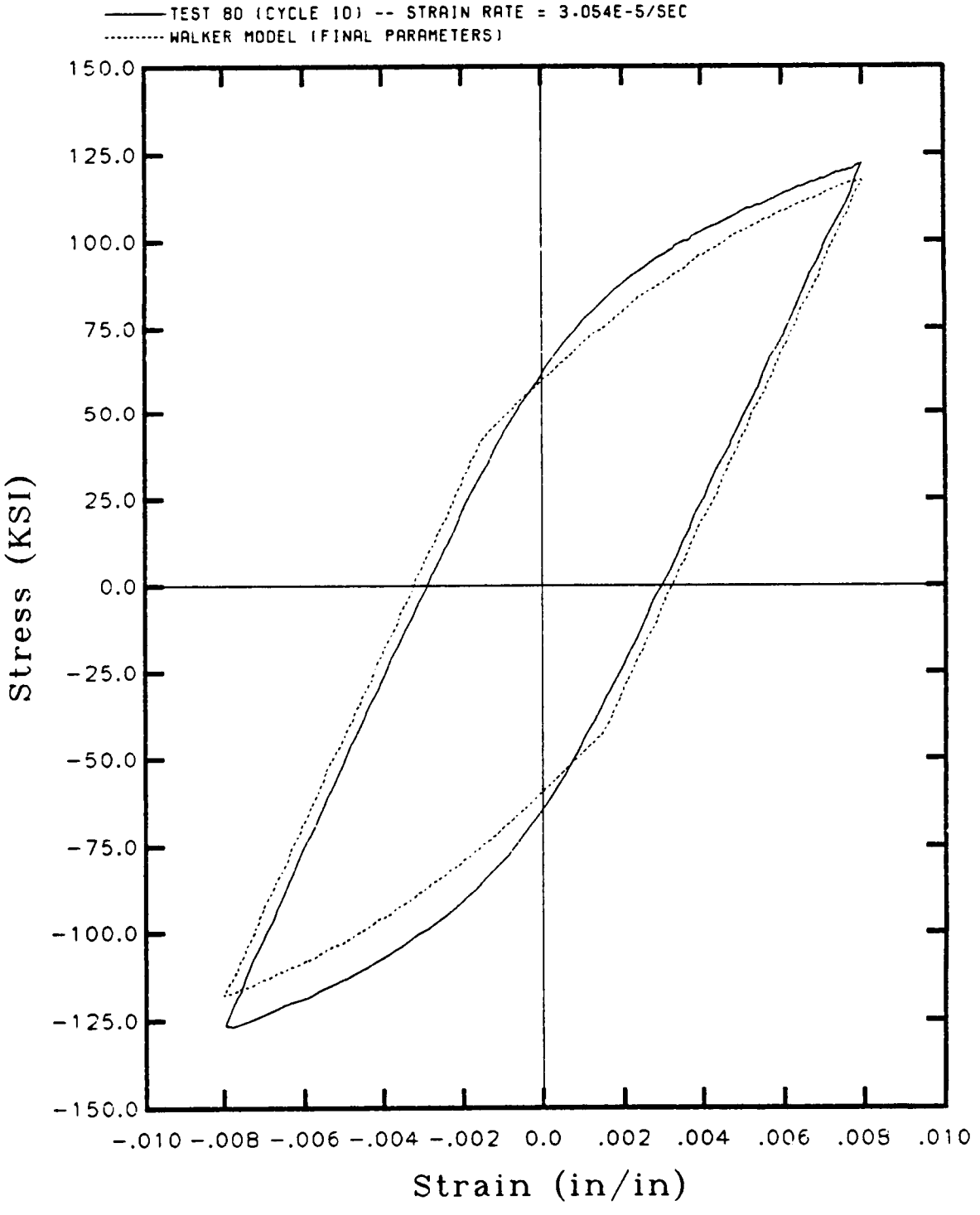

Figure 17. Comparison of Walker's model to the last cycle of Test 80.

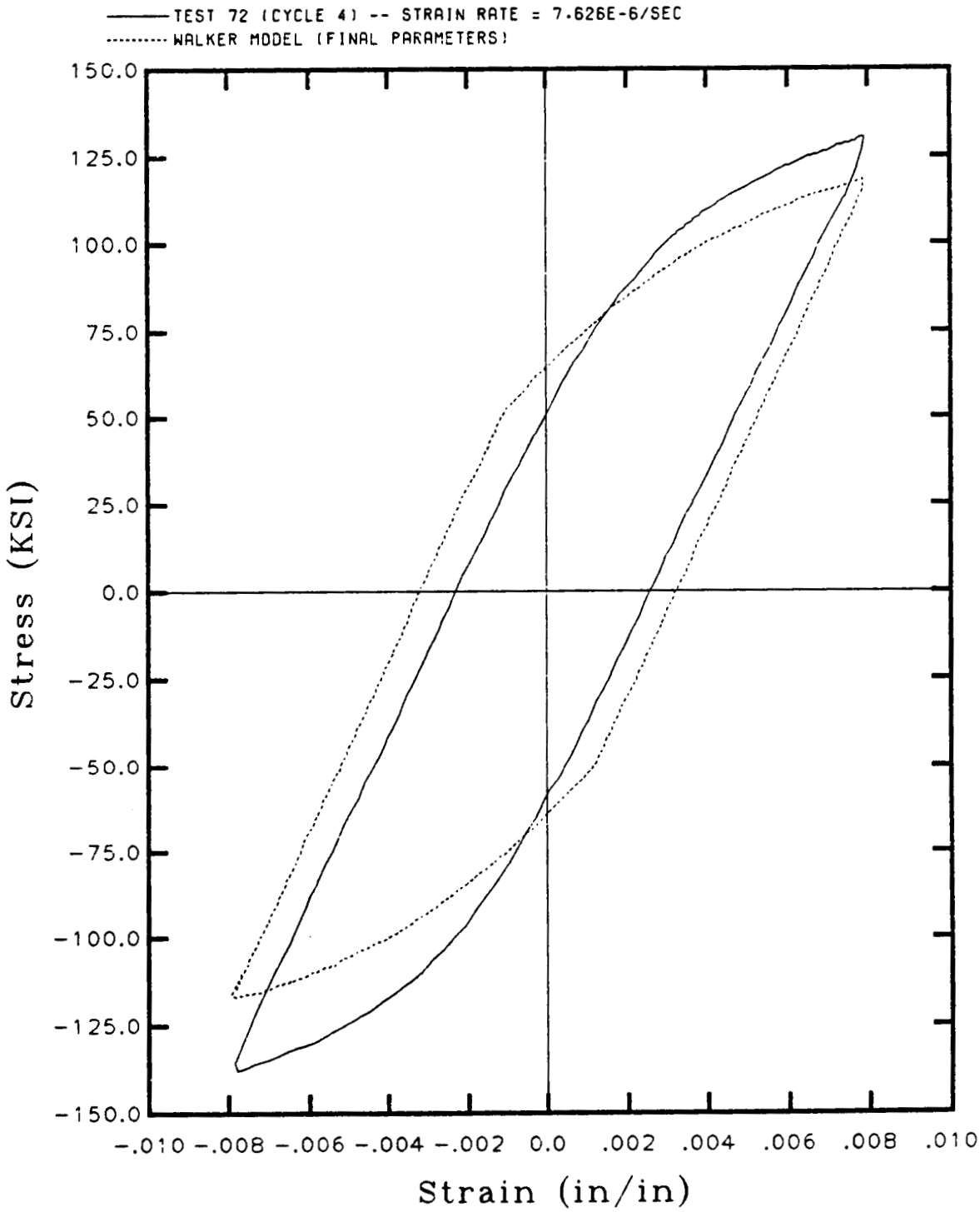

Figure 18. Comparison of Walker's model to the last cycle of Test 72.

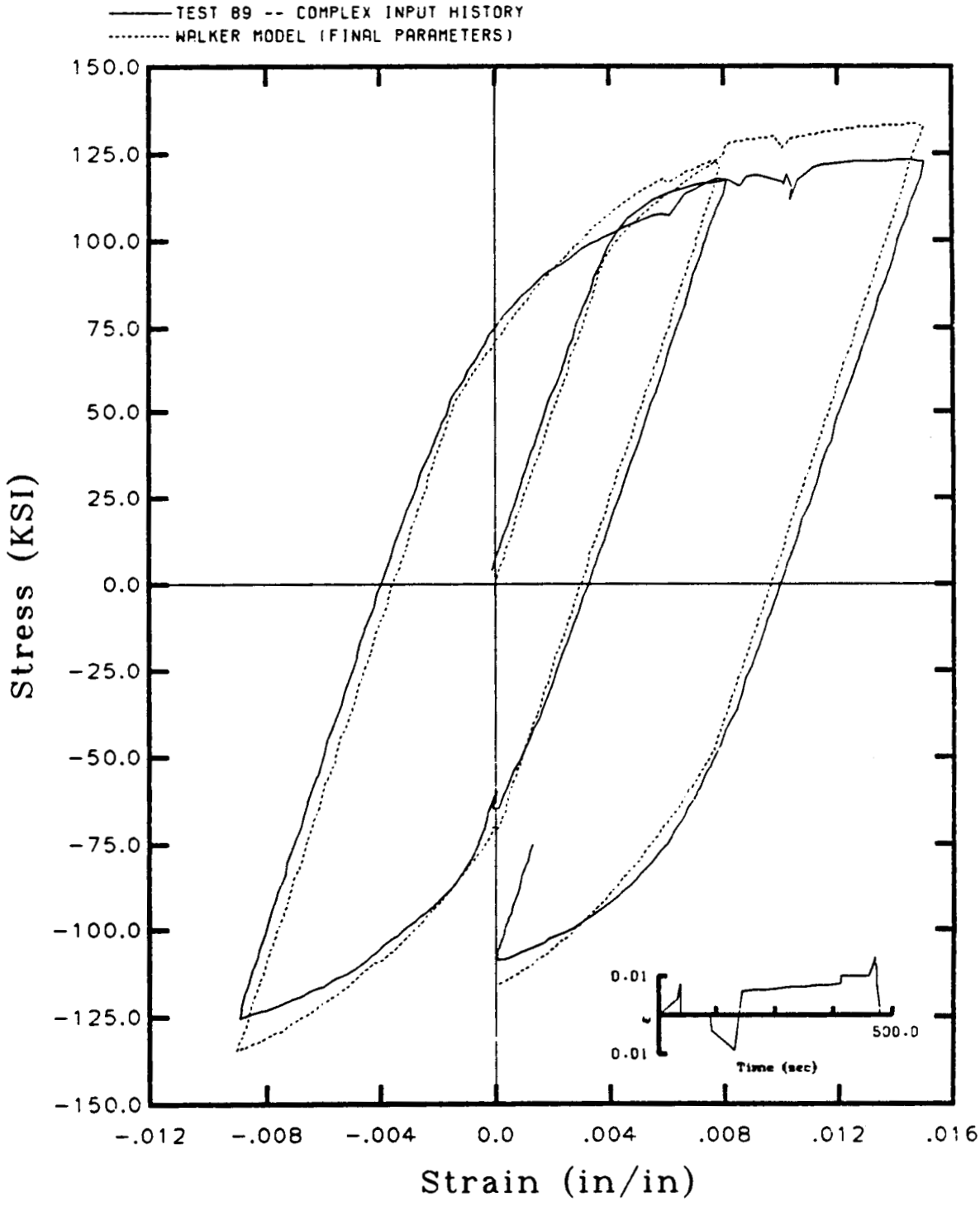

Figure 19. Comparison of Walker's model to a complex history test.